Oxidants Emergence under Dual-Frequency Sonication within Single Acoustic Bubble: Effects of Frequency Combinations

Kerboua, Kaouther*[+•]; Hamdaoui, Oualid

Laboratory of Environmental Engineering, Department of Process Engineering, Faculty of Engineering, Badji Mokhtar - Annaba University, P.O. Box 12, 23000 Annaba, ALGERIA

ABSTRACT: *The sonochemical activity of an oxygen bubble formed in an aqueous medium and oscillating under a dual-frequency excitation is studied in this paper. Several couples of frequencies are formed amongst 35, 140, 300, and 515 kHz, with a maximum acoustic amplitude of 1.5 atm. The molar yields of the emerging oxidants are analyzed in accordance with the combined frequencies and compared to the cases of mono-frequency excitations of similar maximum amplitude, i.e., 1.5 atm. Qualitatively, passing from a mono to a dual-frequency excitation demonstrated to be with no effect on the predominant species which remain $HO^{\bullet}$, $HO_2^{\bullet}$, O and O_3. However, the results exhibited a very selective quantitative evolution depending on the combined frequencies. Some couples proved to induce a negative effect and reduce the production at the single bubble level, particularly with basic frequencies of 140 and 300 kHz, while some others demonstrated a noticeable enhancement such as the couples (35, 140 kHz) and (515, 35 kHz), as compared to mono-frequency fields.*

KEYWORDS: *Dual-frequency; Oxidants; Sonochemical activity; Acoustic cavitation bubble; Kinetics.*

INTRODUCTION

Sonochemical processes knew in last years an exponential evolution; they offer a very wide panoply of applications that hundreds of studies can be found in bibliography. Sonochemical synthesis constitutes an important proportion of these studies. To illustrate, ultrasound-assisted synthesis of nanostructures of mineral oxides has been deeply investigated by *Salavati-Niasari et al.* [1], *Momenian et al.* [2], *Ghanbari et al.* [3] and *Zinatloo-Ajabshir et al.* [4,5]. In such processes, ultrasound proved to act on the morphology and purity of obtained nanoparticles, which constitutes a revolution in synthesizing nanocatalysts such as $NdVO_4$, serving in the activation of some decontamination processes as demonstrated by *Monsef et al.* [6]. Meanwhile, sonochemistry can also be used as an advanced oxidation technique, which remains more promising in wastewater treatment. In this field, numerous studies were elaborated in regards to the effects of the influencing parameters on the harsh conditions attained within the cavitation bubble and consequently on the sonochemical production [7]. The superposition of operating frequencies [8] of the irradiating wave constitutes a new dimension to the

* *To whom correspondence should be addressed.*

+ *E-mail*: *k.kerboua@esti-annaba.dz , kaouther.kerboua.esti@gmail.com*

● *Other Address : Ecole Supérieure de Technologies Industrielles, Department of Second Cycle, P.O. Box 218, 23000 Annaba, ALGERIA*

1021-9986/2021/1/323-332 10/$/6.00

sonochemical reactors [9]. For instance, *Zhang et al.* [10] examined the Bjerknes forces induced between two bubbles under a dual-frequency field, they investigated as well the amplitude of combined and simultaneous resonance of acoustic bubbles [11]. Besides, the multi-frequency systems proved to offer under some conditions an optimal utilization of energy. Indeed, *Gogate et al.* [12], who studied experimentally the sonochemical degradation of formic acid proved that the multiple frequency transducer provides the optimal energy efficiency as compared to mono-frequency horn or bath. Moreover, *Feng et al.* [13] demonstrated in their works that the use of multiple frequency sources could offer a higher cavitation yield. *Sivakumar et al.* [14] confirmed this result through the evaluation of the kinetics of sonochemical degradation of *p*-nitrophenol under a dual-frequency field. In addition, the cavitational volume seems to be improved within the reactor under a dual-frequency excitation. *Moholkar et al.* [15] demonstrated that the dual-frequency sonication allows better control of the cavitation model and the spatial distribution of bubbles inside the reactor. In some other studies, a decrease in the sonochemical activity was noticed when imposing a dual-frequency excitation to the medium. For instance, *Suzuki et al.* [16] demonstrated in their research that combining 20 kHz with a frequency comprised between 200 and 500 kHz induces a decrease in the sonochemical activity, while a synergetic effect appeared with frequencies below 100 kHz.

On the other hand, several attempts to explain the specific effect of dual-frequency excitation on sonochemical activity have been presented in the bibliography. *Suzuki et al.* [16] related the synergetic effect noticed with some couples of frequencies to the increase of the number of cavitation, this result has been proved through the analysis of the acoustic noise spectrum. *Sivakumar et al.* [14] completed their experimental work by a number of simulations in order to figure out the reason behind the observed effect, though the absolute contribution of the dual-frequency field in the chemical kinetics enhancement was difficult to establish, the variation in the rate constants has been explained based on the difference in the acoustic pressure field. Several other authors presented a panoply of explanations of the effect of the dual-frequency sonication on the sonochemical activity. In fact, the previous analysis reveals that most of the pre-cited studies were based on experiments, i.e., the reactor scale and not on the single bubble scale, the present study will be focused on this last axis, using a numerical simulation model.

Two important factors should get special attention, firstly, the nonlinear response of bubble dynamics to the exciting wave, or in other words the instability of bubble dynamics, and secondly, the maximum power provided to the medium when it is exposed to either a mono or a dual-frequency excitation. Both factors can possibly interfere with the effect of the dual-frequency sonication and its interpretation. Thus, we imposed two conditions to ensure stable oscillation of bubble and exposure to comparable maximum acoustic powers, when the bubble is undergoing either a mono or a dual-frequency field, as explained in the following section.

THEORETICAL SECTION

Theory of calculation

In the present study, the bubble is treated as a micro-reactor with a permanent spherical shape. Though the cavitation bubble is supposed to lose its sphericity, especially at the final stages of collapse [17], and due to the strong jet formation [18], it is well accepted to neglect the deviation from the spherical shape in simulation studies [19,20]. The volume of the bubble is changing in function of time according to the variation of the acoustic pressure applied by the ultrasonic wave on the liquid medium at each instant. Due to inertial forces, the bubble undergoes a nonlinear oscillation described by the modified Keller-Miksis equation [21] expressed by the following formula:

$$\ddot{R} = \frac{\dot{c} + \dot{R}}{\rho\left(c\dot{R} - R\dot{R} + \frac{\dot{m}R}{\rho}\right) + 4\mu} \times \left(\left(P_g - \frac{26}{R} - 4\mu\frac{\dot{R}}{R} - P_0 - P_w\left(t + \frac{R}{c}\right)\right)\right) + \frac{R}{\rho\left(c\dot{R} - R\dot{R} + \frac{\dot{m}R}{\rho}\right) + 4\mu}\left(\frac{dP_g}{dt} + \frac{26\dot{R}}{R^2} + 4\mu\frac{\dot{R}^2}{R^2}\right) - \frac{\rho\left(\left(3c - \dot{R}\right) + \frac{2\dot{m}}{\rho}\right)\dot{R}^2}{2\left(\rho\left(c\dot{R} - R\dot{R} + \frac{\dot{m}R}{\rho}\right) + 4\mu\right)} + \frac{\ddot{m}\left(c\dot{R} - R\dot{R} + \frac{\dot{m}R}{\rho}\right)}{\rho\left(c\dot{R} - R\dot{R} + \frac{\dot{m}R}{\rho}\right) + 4\mu} + \frac{\dot{m}\left(c\dot{R} + \frac{\dot{m}}{2\rho}\left(c + \dot{R}\right)\right)}{\rho\left(c\dot{R} - R\dot{R} + \frac{\dot{m}R}{\rho}\right) + 4\mu} \quad (1)$$

$\dot{m}$ represents the mass rate of water molecules due to physical transformations, and $\ddot{m}$ is its time derivate. The modified Keller-Miksis equation considers the non-equilibrium of H_2O mass, due to simultaneous evaporation and condensation of water molecules.

The properties of the excitation wave are the central point of this work. Four frequencies have been selected for the excitation waves: 35, 140, 300, and 515 kHz. These frequencies were chosen for being the most common values retrieved in experimental and numerical studies dealing with sonochemical activity [22–25]. The liquid medium is exposed to a static pressure of 1 atm and an ambient temperature of 20 °C. The mechanical perturbation crossing the liquid medium takes one of the following forms:

$$P_w(t) = -P_A \sin(2\pi f t) \quad \text{for mono-frequency sonication} \tag{2}$$

$$P_w(t) = \frac{-P_A}{2}(\sin(2\pi f_1 t) + \sin(2\pi f_2 t + \phi)) \quad \text{for dual-frequency sonication} \tag{3}$$

The dual-frequency field is expressed as a sum of two synchronized sinusoidal signals of respective frequencies f_1 and f_2. ϕ represents the phase difference between both waves. In this study, we opt for a null delay in the irradiation by both signals, with respects to the results of *Tatake* and *Pandit* [26] who demonstrated a maximum sonochemical efficiency in the absence of a phase difference. For accommodation purposes, "basic frequency" is used to qualify the frequency of the wave that forms initially a mono-frequency excitation. When another wave is superposed to the basic one to form a dual-frequency field, the frequency of this last wave is noted as "the second frequency".

The acoustic amplitude P_a was fixed at 1.5 atm, both waves composing the dual-frequency field are characterized by a similar maximum amplitude that equals $\frac{P_a}{2}$ [27–29]. Consequently, the maximum acoustic amplitude exerted by a mono-frequency wave is equivalent to that due to the dual-frequency sonication. This choice permits to explain the frequencies association effect without the interference of the acoustic pressure amplification. Additionally, at this particular value of acoustic amplitude, it was possible to find a common ambient radius value located in the stable and active zone on the shape stability diagrams [22,30–33] at each one of the aforementioned frequencies. Hence, 2 µm is selected as the initial bubble radius corresponding to the time origin at which the medium starts to be irradiated, in order to avoid a non-uniform dynamical behavior [34,35] that would be explained by bubble instability [36,37] at one of the previous conditions. In accordance with previous criteria, the studied bubble corresponds to a "high energetic stable bubble" [38].

In addition to oscillation dynamics, mass and energy balances of the bubble are established, assuming that the spherical reactor is an open system for mass and heat exchange. The parameters describing the state of the bubble are related through the Van der Waals equation. Pressure and temperature within the bubble are considered to be uniform within its volume. Temperature variation in the function of time is governed by an energy balance, given in the following equation:

$$\frac{1}{nC_V}(-P_g dV(t) - \sum_{i=1}^{25} \Delta H_i r_i V(t) dt + S(t)\frac{m}{M} C_{V_{H2O}} T dt) = \frac{\lambda}{\xi n C_V} 4\pi R^2 (T - T_\infty) dt + dT \tag{4}$$

The bubble contains initially a mixture of water vapor and oxygen. The water vapor is due to its saturating vapor pressure at the operational conditions, given by Antoine's equation:

$$\ln(P_{H2O}/133.32) = 18.3036 - \frac{3816.44}{T - 46.13} \tag{5}$$

The H_2O molecules undergo a mass transfer from and into the bubble as a result of the non-equilibrium of evaporation and condensation. The molar rate involved in this phenomenon is expressed by Hertz-Knudsen law [39]:

$$\dot{n} = \frac{1}{\sqrt{2\pi M R_g}} \alpha \frac{1}{\sqrt{T}} (P_v - P_{H2O}) \tag{6}$$

where α is the accommodation coefficient, expressed through Gregory-Newton Formula [21].

The water and oxygen molecules initially present in the bulk of the bubble interact according to a set of chemical reactions expected to occur inside the bubble during the collapse. The details of this chemical schema are given in a previous study [40]. This interaction induces the emergence of a number of oxidants such as H_2O_2, $HO^\bullet$

and $HO_2^{\bullet}$. The variation of the mass of each reactant or product is the result of chemical and physical kinetics according to the equations below:

$$\dot{c}_i = \dot{c}_i^{ph} + \dot{c}_i^{ch} \quad (7)$$

$$\dot{c}_i^{ch} = \sum_{i=1}^{25} \vartheta_{li} \left(k_{fi}(T) \prod_{j=4}^{12} \left[c_j\right]^{\vartheta_{ij}} - k_{ri}(T) \prod_{j=4}^{12} \left[c_j\right]^{\vartheta'_{ij}} \right) - \quad (8)$$

$$3 \times c_i \times \frac{\dot{R}}{R}$$

$$\dot{c}_{H_2O}^{ph} = -3 \frac{1}{R\sqrt{2\pi M_{H_2O} R_g}} \alpha (P_v - P_{H_2O}) \quad (9)$$

$$\dot{c}_i^{ph} = 0 \quad for\ i \neq H_2O$$

The whole set of phenomena interacting in the activity of the acoustic cavitation bubble is translated into a complex system of nonlinear differential equations, resolved numerically using the 4th-order Runge-Kutta algorithm. The simulations are conducted on a duration of 100 µs that proved to be sufficient to obtain representative dynamical response of the bubble to the excitation field, and offering convenient readability, especially at short periods, i.e., under 300 and 515 kHz. The resolution of this system offers a quantity of data regarding the bubble dynamics, the temperature and pressure inside the bubble, and the mass variation all along with the bubble oscillation. The present work is focused on this last axis, by analyzing the mass evolution, the species predominance, and the sonication efficiency when a single bubble is undergoing either a mono or a dual-frequency excitation.

RESULTS AND DISCUSSION

The computational simulations conducted in this study consisted of a numerical resolution of a system of non-linear dependent differential equations and returned, among others, the time variations of the molar yields of the nine species involved in the chemical mechanism during the simulation time. The discussion of the data collected from the numerical simulation is split into three parts. Firstly, we proceed with the qualitative characterization of the chemical products in order to identify the predominant ones in the function of the exciting field. Secondly, we examine the effect of the combined frequencies on the evolution of the total molar production as well as the molar yields of major emerging products. Thirdly and finally, we identify the couples leading to synergetic effect and attempt to explain the action mechanism of dual-frequency excitation.

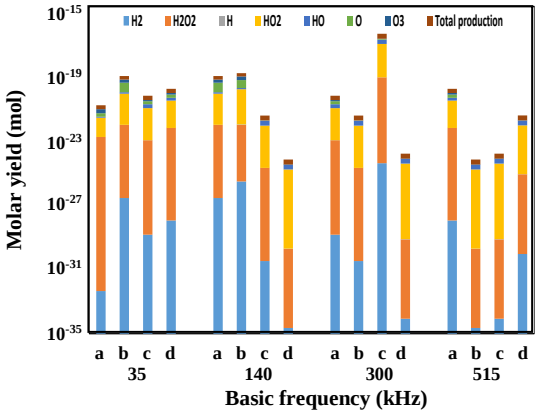

Fig. 1: Molar yields of different products and overall sonochemical production under various cases of mono and dual-frequency excitations resulting of the association of a basic frequency to 35 kHz (a), 140 kHz (b), 300 kHz (c), and 515 kHz (d).

In this section, the major products are identified according to their proportions by the end of simulation time, i.e., 100 µs. The comparison of the molar quantities of the seven emerging species is reported in Fig.1, it demonstrates that $HO^{\bullet}$, $HO_2^{\bullet}$, O and O_3 remain predominant under all the studied cases of mono and dual-frequency excitations. However, their molar fractions depend on a couple of frequencies: with relatively low basic frequencies, i.e., 35 and 140 kHz, the production of O is promoted, it covers for instance 23% to 47% of the total production under a basic frequency of 35 kHz. In contrast, with relatively high basic frequencies, i.e., 300 and 515 kHz, the production of $HO^{\bullet}$ and $HO_2^{\bullet}$ takes the upper hand. At the end of simulation time, these two free radicals are present in very close molar fractions, attaining 50% of the total production for each species under the couples (515, 140 kHz) and (515, 300 kHz). It is also worthy to note that with any of the four basic frequencies treated in this study, the lower the second frequency, the higher the proportion of O at the expense of $HO^{\bullet}$.

As a second step, the molar yields of the four predominant products are analyzed according to the excitation wave and are reported in Fig. 2. The variation of the quantities of $HO^{\bullet}$, $HO_2^{\bullet}$, O and O_3 seem to follow similar trends in the function of the excitation field. With a basic frequency of 35 kHz, these trends show a noticeable

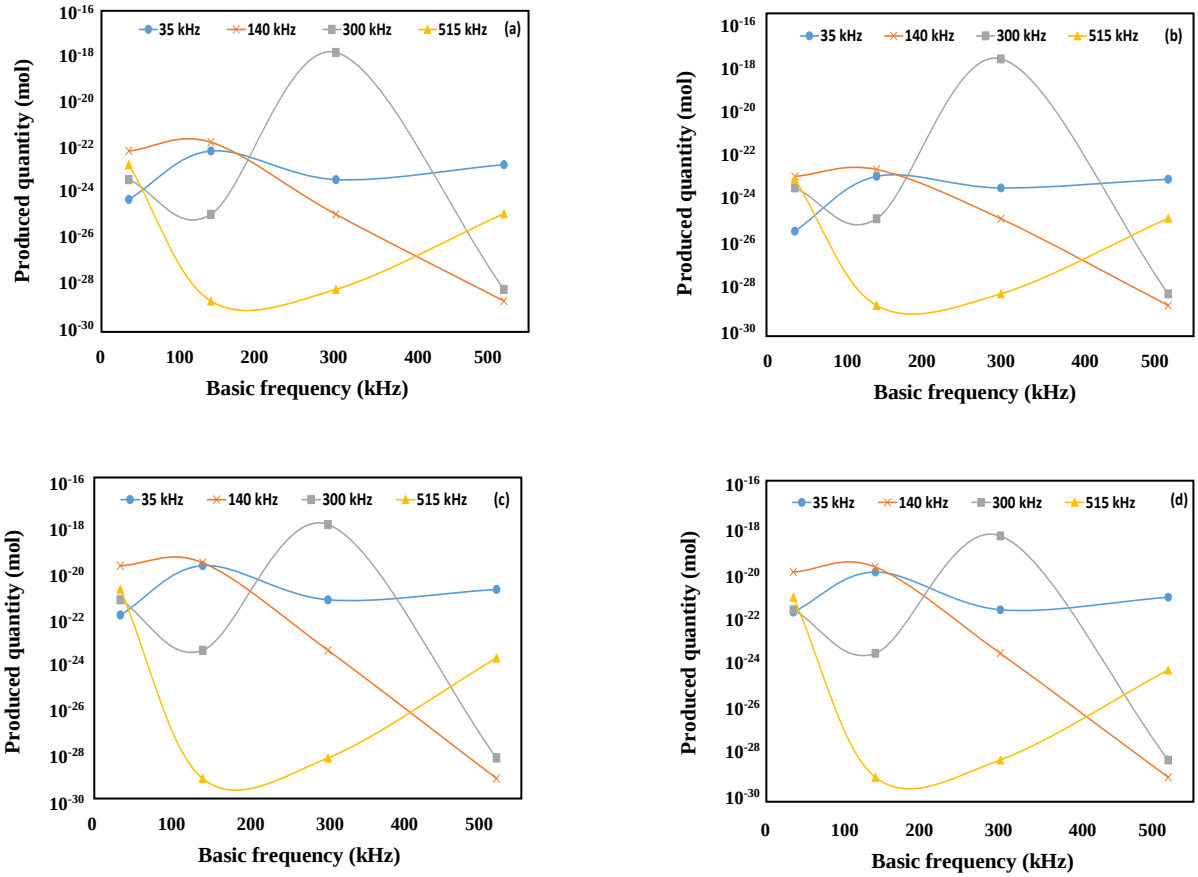

Fig. 2: Molar yields variations of $HO_2^{\bullet}$ (a), $OH^{\bullet}$ (b), O (c) and O_3 (d) in the function of mono and dual-frequency excitations.

enhancement when passing from the mono to the dual-frequency excitation, the maximum enhancement ratio is attained when coupling 35 to 140 kHz, it reaches 31 for $HO_2^{\bullet}$, 48 for $HO^{\bullet}$, 55 for O_3 and 135 for O. At the opposite, with a basic frequency of 140 kHz, the maximum productions of the four predominant species are recorded under the mono-frequency sonication. Associating 140 kHz with 35, 300, or 515 kHz induces a decrease in the molar yields of $HO^{\bullet}$, $HO_2^{\bullet}$, O and O_3. This negative effect attains its maximum with the couple (140, 515 kHz), indeed, in this case, the molar quantities know a drastic drop with a magnitude varying from 10^5 to 10^{10}. A basic frequency of 300 kHz results in an identical behavior as with 140 kHz, the mono-frequency excitation results in the highest molar production, and its association with a second frequency leads to an important reduction of molar quantities, especially with the couples (300, 35 kHz) and (300, 515 kHz). Under a basic frequency of 515 kHz, the association with the second frequency of 35 kHz is the only case conducting better results than that of the mono-frequency excitation. Enhancement ratios of 1484, 914, 32, and 16 are retrieved for the molar yields of O_3, O, $HO_2^{\bullet}$ and $HO^{\bullet}$, respectively.

The overall sonochemical production at a single bubble level is reported as well in Fig. 1 for the various cases of mono and dual-frequency excitations. First of all, we notice that 300 kHz sonication leads to the most important products among the mono-frequency excitation cases, with almost 1.08×10^{-17} mol, followed by 140 kHz with 3.20×10^{-20} mol. These values are equivalent to average rates of production of 65000 and 193 molecules/bubble·µs, respectively. The optimum production encountered at 300 kHz could be explained by the competition of two phenomena: the evolution of chemical kinetics and the loss of water molecules due to condensation at the bubble wall. Indeed, the increase of ultrasonic frequency is accompanied of a decrease in extreme values of pressure and temperature attained at the bubble collapse [41], which

is supposed to curb the chemical kinetics. Simultaneously, a non-equilibrium of evaporation and condensation of water, molecules occur at the bubble wall. Although the condensation takes the upper hand, this phenomenon is attenuated by the increase of frequency [39], which provides higher reactant quantities. The compromise between the resulting amount of water molecules and their conversion rate in function of the acoustic frequency makes 300 kHz the optimum condition for sonochemical production.

In both previous cases, i.e., at 300 and 140 kHz, it seems that passing to dual-frequency excitation is of a negative effect on the sonochemical production, as compared to mono-frequency excitation. On the opposite, an enhancement of the overall production was observed when coupling 35 kHz to 140, 300, and 515 kHz, the maximum production was recorded with the couple (35, 140 kHz). With 515 kHz, the only case of dual-frequency excitation showing an increase of production, as compared to the mono-frequency excitation, is that of coupling to 35 kHz.

The synergetic effect of dual-frequency excitation in terms of sonochemical production was questioned in this paper. In other words, the molar yields of major oxidants obtained under dual-frequency excitation were compared to the outcomes of mono-frequency waves composing the couple, and exerting the same maximum power on the medium. The results of this comparison proved that among the ten cases covered by this study, only the couple (35, 515 kHz) is believed to be more interesting than each one of the mono-frequencies composing it, as shown in Fig. 3. With all the other couples, even those showing an enhancement as compared to the production of a basic frequency, the obtained molar yield appeared to have an intermediate value between those resulting from the mono-frequency excitation with the basic and the second frequencies are treated separately.

In an attempt to explain this selective behavior, the previous trends were analyzed in accordance with dynamics [29] and energetic parameters [42]. With basic frequencies of 35 and 515 kHz, the overall sonochemical production is closely linked to the evolution of the maximum temperature. Indeed, with a basic frequency of 35 kHz, the highest T_{max} is encountered with the couple (35, 140 kHz) and equals 4600 K, while the mono-frequency sonication leads to approximately 4100 K only, which is in a good correlation with the evolution of the molar

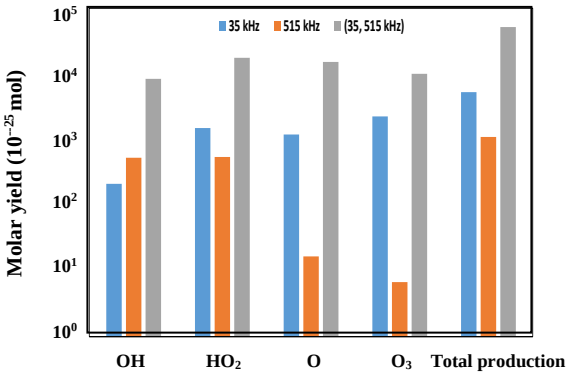

Fig. 3: Molar yields of the four predominant products and overall sonochemical production under mono-frequency excitations of 35 and 515 kHz, and under a dual-frequency excitation associating both frequencies.

production. Similarly, with a basic frequency of 515 kHz, T_{max} reaches its maximum under a dual-frequency sonication associating 515 to 35 kHz, with a value of 3600 K.

With basic frequencies of 140 and 300 kHz, though a noticeable enhancement of maximum temperature was retrieved when coupling both previous values with lower frequencies, no increase in sonochemical production was recorded. With both previous frequencies, the highest maximum temperatures recorded at the strong collapse correspond to the couples (35, 140 kHz) and (35, 300 kHz), respectively. In both cases, T_{max} exceeds the orders of magnitude of 4600 and 3300 K, while it is limited to 4400 and 3000 K under mono-frequency excitations, which is equivalent to relative increases of 4.5 and 10%. Hence, T_{max} is not the major parameter acting on the chemical kinetics, the sonochemical production depends as well on the collapse phase duration and the occurrence of harsh conditions within it. Hence, the effect of frequency combinations on the sonochemical activity should be rigorously examined case by case, nevertheless, it is rather positive when thermal conditions are improved during the collapse and harsh collapses occur frequently during the bubble lifetime, what happens, in this case, is equivalent to controlled pulsed sonication. The combinations leading to negative effects are possibly explained by either the diminution of harsh temperature and pressure values or the limited occurrence of violent conditions during the simulation time. It is important to note as well that the limit at which we can consider the bubble as “sonochemically active”, fixed

Table 1: Bibliographic review of dual-frequency effect on the sonochemical activity.

Authors	Comparison reference	Experimental conditions	Acoustic conditions	f_1	f_2	Combination effect $f_1 \Rightarrow (f_1,f_2)$
Sivakumar et al. [14]	Degradation of p-nitrophenol	V_R=1500 mL C_0=10 ppm; 150 min	25 kHz, 120 W (25, 40 kHz), 240 W	25 kHz	40 kHz	10% ⇒ 26%
Lee and Oh [27]	Emergence of Hydrogen peroxide from water	V_R=3900 mL 60 min	28 kHz, 150 W (28, 970 kHz), 300 W	28 kHz	970 kHz	0.30 ppm ⇒ 1.30 ppm
Suzuki et al. [16]	Emergence of triiodide from Potassium Iodide	V_R=1000 mL C_0=0.1 M; 10 min	50 kHz, 40 W (50, 20 kHz), 60 W	50 kHz	20 kHz	0.20 µmol ⇒ 1.80 µmol
			100 kHz, 40 W (100, 20 kHz), 60 W	100 kHz	20 kHz	7.10 µmol ⇒ 7.10 µmol
			200 kHz, 40 W (200, 20 kHz), 60 W	200 kHz	20 kHz	10.30 µmol ⇒ 8.60 µmol
			450 kHz, 40 W (450, 20 kHz), 60 W	450 kHz	20 kHz	10.20 µmol ⇒ 8.00 µmol
Gogate et al. [12]	Degradation of formic acid	V_R=1500 mL C_0=1000 ppm; 120 min	20 kHz, 120 W (20, 30 kHz), 240 W	20 kHz	30 kHz	2.2% ⇒ 3.7%
			20 kHz,120 W (20, 50 kHz), 240 W	20 kHz	50 kHz	2.2% ⇒ 3.8%
			25 kHz,120 W (25, 40 kHz), 240 W	25 kHz	40 kHz	5.5% ⇒ 6.5%
			30 kHz,120 W (30, 50 kHz), 240 W	30 kHz	50 kHz	2.6% ⇒ 4.9%

conventionally at a single bubble scale to 10^8 molecules/second [30], was exceeded only in three cases: under mono-frequency excitations of 140 and 300 kHz and under the couple (35, 140 kHz). This fact questions the sonochemical efficiency of coupling frequencies, as the only case that appeared to be quantitatively interesting, i.e., the couple (35, 515 kHz), does not attain the barrier of sonochemical activity. Besides, the production enhancement observed in some cases under a dual-frequency field at a reactor scale, such as in the studies of *Sivakumar et al.* [14], *Lee* and Oh [27], and *Gogate et al.* [12] reported in Table 1, would be partially explained by the sonochemical activity improvement at a single bubble level. However, the modification of the distribution and the number of bubbles within the reactor could better explain the observed effect, as reported in some previous papers, especially that the synergetic effect seems to be very limited at a single bubble scale.

CONCLUSIONS

The present work constitutes a numerical study of the effect of dual-frequency sonication on the sonochemical activity of a very specific type of bubble. Conditions were selected to deal with stable oscillating bubbles, undergoing similar maximum powers when they are exposed to either mono or dual-frequency excitations. The sonochemical production was quantified and predominant species were identified among the seven emerging products. The results proved that in all the cases, the relative prevalence of oxidants was conserved, O_3, O, $HO_2^{\bullet}$ and $HO^{\bullet}$ were the major products. Moreover, these four species showed similar trends of molar yields variation in function of the exciting field. In terms of molar quantities, passing from mono-frequency excitations of 140 and 300 kHz to dual-frequency demonstrated a negative effect with all the formed couples. On the opposite, associating 35 kHz to 140 kHz conducted to a noticeable enhancement with an order of magnitude exceeding 50 times. With a basic frequency of 515 kHz, the overall production, as well as the molar yields of the predominant products, were highly improved with the couple (515, 35 kHz). This last case was the only one resulting in a synergetic effect, though producing a quantity lower than the barrier of considerable sonochemical activity. Finally, it is worthy to note that the positive effect of the dual-frequency sonication observed at the reactor scale regarding the sonochemical production would be rather assigned to the modification of the bubble distribution and number than to the production at a single

bubble scale. Hence, the numerical investigation of the activity of the sonochemical reactor, or in other words the bubble population, remains the key to explain accurately the effect of multi-frequency excitation, however, this needs the consideration of several parameters such as bubble-bubble interactions [43], space distribution [44] and wave attenuation [45].

Nomenclature

μ	Dynamic viscosity, Pa s
ρ	Density, kg/m^3
σ	Surface tension, N/m
α	Accommodation coefficient
ΔH_i	Reaction heat of the ith reaction, J/mol
c	Sound celerity, m/s
f	Frequency, Hz
M	Molar mass, kg/mol
m	Mass flow of water, kg/m^2
$\dot{m}$	Evaporation-condensation rate of water, kg/m^2 s
n	Molar amount, mol
n_0	Initial molar amount, mol
$\dot{n}$	Evaporation-condensation rate of water, mol/ m^2 s
P_A	Acoustic amplitude, Pa
P_{H2O}	Saturating vapor pressure, Pa
P_v	Vapor pressure, Pa
P_w	Pressure of the wave travelling the medium, Pa
R	Bubble radius, m
$\dot{R}$	Bubble wall velocity, m/s
$\ddot{R}$	Bubble wall acceleration, m/s^2
r_i	Reaction rate of the ith reaction, mol/s m^3
R_g	Ideal gas constant, J/mol K
S	Section of the bubble wall, m^2
T	Temperature within the bubble, K
t	Time, s
V	Volume of the bubble, m^3
V_R	Reactional volume, mL

Received : Jun. 17, 2019 ; Accepted : Sep. 16, 2019

REFERENCES

[1] Salavati-Niasari M., Javidi J., Davar F., Sonochemical Synthesis of Dy2(CO3)3 Nanoparticles, Dy(OH)3 Nanotubes and their Conversion to Dy2O3 Nanoparticles, *Ultrason. Sonochemistry*, **17**: 870–877(2010). doi:10.1016/j.ultsonch.2010.02.013.

[2] Momenian H.R., Gholamrezaei S., Salavati-Niasari M., Pedram B., Mozaffar F., Ghanbari D., Sonochemical Synthesis and Photocatalytic Properties of Metal Hydroxide and Carbonate (M:Mg, Ca, Sr or Ba) Nanoparticles, *J. Clust. Sci.*, **24**: 1031–1042 (2013). doi:10.1007/s10876-013-0595-y.

[3] Ghanbari D., Salavati-Niasari M., Ghasemi-Kooch M., A sonochemical Method for Synthesis of Fe_3O_4 Nanoparticles and Thermal Stable PVA-Based Magnetic Nanocomposite, *J. Ind. Eng. Chem.*, **20**: 3970-3974 (2014). doi:10.1016/j.jiec.2013.12.098.

[4] Zinatloo-Ajabshir S., Salavati-Niasari M., A Sonochemical-Assisted Synthesis of Pure Nanocrystalline Tetragonal Zirconium Dioxide Using Tetramethylethylenediamine, *Int. J. Appl. Ceram. Tec.*, **662**: 654-662 (2014). doi:10.1111/ijac.12269.

[5] Zinatloo-Ajabshir S., Mortazavi-Derazkola S., Salavati-Niasari M., Nd_2O_3-SiO_2 Nanocomposites: A Simple Sonochemical Preparation, Characterization and Photocatalytic Activity, *Ultrason. Sonochem*,**42**: 171–182 (2018). doi:10.1016/j.ultsonch.2017.11.026.

[6] Monsef R., Ghiyasiyan-Arani M., Salavati-Niasari M., Application of Ultrasound-Aided Method for the Synthesis of $NdVO_4$ Nano-Photocatalyst and Investigation of Eliminate Dye in Contaminant Water, *Ultrason. Sonochem*, **42**: 201–211 (2018). doi:10.1016/j.ultsonch.2017.11.025.

[7] Wood R.J., Lee J., Bussemaker M.J., A Parametric Review of Sonochemistry: Control and Augmentation of Sonochemical Activity In Aqueous Solutions, *Ultrason. Sonochem*, **38**: 351–370 (2017). doi:10.1016/j.ultsonch.2017.03.030.

[8] Brotchie A., Mettin R., Grieser F., Ashokkumar M., Cavitation Activation by Dual-Frequency Ultrasound and Shock Waves, *Phys. Chem. Chem. Phys.*, **11**: 10029–10034(2009). doi:10.1039/b912725a.

[9] Kanthale P.M., Gogate P.R., Pandit A.B., Modeling Aspects of Dual Frequency Sonochemical Reactors, *Chem. Eng. J.*. **127**: 71–79 (2007). doi:10.1016/j.cej.2006.09.023.

[10] Zhang Y., Zhang Y., Li S., The Secondary Bjerknes Force Between Two Gas Bubbles Under Dual-Frequency Acoustic Excitation, *Ultrason. Sonochem*, **29**: 129–145 (2016). doi:10.1016/j.ultsonch.2015.08.022.

[11] Zhang Y., Zhang Y., Li S., Combination and Simultaneous Resonances of Gas Bubbles Oscillating in Liquids under Dual-Frequency Acoustic Excitation, *Ultrason. Sonochem.*, **35**: 431–439 (2017). doi:10.1016/j.ultsonch.2016.10.022.

[12] Gogate P.R., Mujumdar S., Pandit A.B., Sonochemical Reactors for Waste Water Treatment: Comparison using Formic Acid Degradation as a Model Reaction, *Adv. Environ. Res.*, **7**: 283–299 (2003). doi:10.1016/S1093-0191(01)00133-2.

[13] Feng R., Zhao Y., Zhu C., Mason T.J., Enhancement of Ultrasonic Cavitation Yield By Multi-Frequency Sonication, *Ultrason. Sonochem.*, **9**: 231–236 (2002). doi:10.1016/S1350-4177(02)00083-4.

[14] Sivakumar M., Tatake P.A., Pandit A.B., Kinetics of p-nitrophenol Degradation: Effect of Reaction Conditions and Cavitational Parameters for a Multiple Frequency System, *Chem. Eng. J.*, **85**: 327–338 (2002). doi:10.1016/S1385-8947(01)00179-6.

[15] Moholkar V.S., Rekveld S., Warmoeskerken M.M.C.G., Modeling of the Acoustic Pressure Fields and the Distribution of the Cavitation Phenomena in a Dual Frequency Sonic Processor, *Ultrason*, **38**: 666–670 (2000). doi.org/10.1016/S0041-624X(99)00204-8.

[16] Suzuki T., Yasui K., Yasuda K., Iida Y., Tuziuti T., Torii T., Nakamura M., Effect of Dual Frequency on Sonochemical Reaction Rates, *Res. Chem. Intermed.*, **30**: 703–711 (2004). doi:10.1163/1568567041856873.

[17] Mettin R., Cairos C., Troia A., Sonochemistry and Bubble Dynamics, *Ultrason. Sonochem.*, **25**: 24–30 (2015). doi:10.1016/j.ultsonch.2014.08.015.

[18] Zhang Y., Chen F., Zhang Y., Zhang Y., Du X., Experimental Investigations of Interactions Between a Laser-Induced Cavitation Bubble and a Spherical Particle, *Exp. Therm. Fluid Sci.*, **98**: 645-661 (2018). doi:10.1016/j.expthermflusci.2018.06.014.

[19] Prosperetti A., Modelling of Spherical Gas Bubble Oscillations and Sonoluminescence, *R. Soc.*, **357**: 203–223 (1999). doi: 10.1098/rsta.1999.0324

[20] Hickling R., Plesset M.S., The Collapse of a Spherical Cavity in a Compressible Liquid, Report No. 85-24, California Institute of Technology, Pasadena, CA.

[21] Yasui K., Alternative Model of Single Bubble Sonoluminescence, *Phys. Rev. E.*, **56**: 6750–6760 (1997). doi:10.1103/PhysRevA.65.054304.

[22] Yasui K., Influence of Ultrasonic Frequency on Multibubble Sonoluminescence, *Acoust. Soc. Am.*, **112**: 1405–1413 (2002). doi:10.1121/1.1502898.

[23] Tuziuti T., Effect of Particle Addition on Sonochemical Reaction, *Ultrasonics*,**42**: 597–601 (2004). doi:10.1016/j.ultras.2004.01.082.

[24] Price G.J., Harris N.K., Stewart A.J., Direct Observation of Cavitation Fields at 23 and 515 kHz, *Ultrason. Sonochem*, **17**: 30–33 (2010). doi:10.1016/j.ultsonch.2009.04.009.

[25] Merouani S., Hamdaoui O., Rezgui Y., Guemini M., Computational Engineering Study of Hydrogen Production *via* Ultrasonic Cavitation in Water, *Int. J. Hydrogen Energy.*, **41**: 832–844 (2016). doi:10.1016/j.ijhydene.2015.11.058.

[26] Tatake P.A., Pandit A.B., Modelling and Experimental Investigation into Cavity Dynamics and Cavitational Yield: Influence of Dual Frequency Ultrasound Sources, *Chem. Eng. Sci.*, **57**: 4987–4995 (2002). doi:10.1016/S0009-2509(02)00271-3.

[27] Lee M., Oh J., Synergistic Effect of Hydrogen Peroxide Production and Sonochemiluminescence Under Dual Frequency Ultrasound Irradiation, *Ultrasonics. Sonochem.*, **18**: 781–788 (2011). doi:10.1016/j.ultsonch.2010.11.022.

[28] Guédra M., Inserra C., Gilles B., *J.C. Béra*, Numerical Investigations of Single Bubble Oscillations Generated by a Dual Frequency Excitation, *J. Phys. Conf. Ser.*, **656**: 1-4(2015). doi:10.1088/1742-6596/656/1/012019.

[29] K. Kerboua, O. Hamdaoui, Numerical Investigation of The Effect of Dual Frequency Sonication on Stable Bubble Dynamics, *Ultrason. Sonochem.*, **49**: 325–332 (2018). doi:10.1016/j.ultsonch.2018.08.025.

[30] Yasui K., Tuziuti T., Lee J., Kozuka T., Towata A., Iida Y., The Range of Ambient Radius for an Active Bubble in Sonoluminescence and Sonochemical Reactions, *J. Chem. Phys.*, **184705**: 1-12(2012). doi:10.1063/1.2919119.

[31] Toegel R., Lohse D., Phase Diagrams for Sonoluminescing Bubbles: A Comparison Between Experiment and Theory, *J. Chem. Phys.*, **118**: 1863–1875 (2003). doi:10.1063/1.1531610.

[32] Pankaj, Ashokkumar, Muthupandian, "Theoretical and Experimental Sonochemistry Involving Inorganic Systems", Springer, (2011). doi: 10.1007/978-90-481-3887-6

[33] Hilgenfeldt S., Lohse D., Brenner M.P., Phase Diagrams for Sonoluminescing Bubbles, *Phys. Fluids.*, **8**: 2808–2826 (1996). doi:10.1063/1.869131.

[34] Zhang Y., Zhang Y., Chaotic Oscillations of Gas Bubbles under Dual-Frequency Acoustic Excitation, *Ultrason. Sonochem.*, 1–6 (2017). doi:10.1016/j.ultsonch.2017.03.058.

[35] Diaz De La Rosa M.A., Husseini G.A., Pitt W.G., Comparing Microbubble Cavitation at 500 kHz and 70 kHz Related to Micellar Drug Delivery Using Ultrasound, *Ultrasonics*, **53**: 377–386 (2013). doi:10.1016/j.ultras.2012.07.004.

[36] Calvisi M.L., Lindau O., Blake J.R., Szeri A.J., Blake J.R., Shape stability and Violent Collapse of Microbubbles in Acoustic Traveling Waves, *Phys. Fluids.*, **047101**: 1-15 (2011). doi:10.1063/1.2716633.

[37] Suzuki H., Lee I.S., Okuno Y., Stability and Dancing Dynamics of Acoustic Single Bubbles in Aqueous Surfactant Solution, *Int. J. Phys. Sci.*, **5**: 176–181 (2010).

[38] Yasui K., Fundamentals of Acoustic Cavitation and Sonochemistry, in: "Theor. Exp. Sonochemistry Involv. Inorg. Syst.", National Institute of Advanced Industrial Science and Technology, Anagahora-Japan, pp. 1–29 (2011). doi:10.1007/978-90-481-3887-6.

[39] Kerboua K., Hamdaoui O., Ultrasonic Waveform Upshot on Mass Variation within Single Cavitation Bubble: Investigation of Physical and Chemical Transformations, *Ultrason. Sonochem.*, **42**: 508–516 (2018). doi:10.1016/J.ULTSONCH.2017.12.015.

[40] Kerboua K., Hamdaoui O., Influence of Reactions Heats on Variation of Radius, Temperature, Pressure and Chemical Species Amounts within a Single Acoustic Cavitation Bubble, *Ultrason. Sonochem.*, **41**: 449–457 (2018). doi:10.1016/j.ultsonch.2017.10.001.

[41] Kerboua K., Hamdaoui O., Computational study of State Equation Effect on Single Acoustic Cavitation Bubble's Phenomenon, *Ultrason. Sonochem.*, **38**: 174–188 (2017). doi:10.1016/j.ultsonch.2017.03.005.

[42] Kerboua K., Hamdaoui O., Acoustic cavitation Bubble under Dual-Frequency Excitation: An Energetic Reading, *Arab. J. Sci. Eng.* (2019).

[43] Yasui K., Iida Y., Tuziuti T., Kozuka T., Towata A., Strongly Interacting Bubbles under an Ultrasonic Horn, *Phys. Rev. E.*, **77**: 1–10 (2008). doi:10.1103/PhysRevE.77.016609.

[44] Mettin R., Koch P., Lauterborn W., Krefting D., "Modeling Acoustic Cavitation with Bubble Redistribution", *Int. Symp. Cavitation.* (2006).

[45] Zhang Y., Guo Z., Du X., Wave Propagation in Liquids with Oscillating Vapor-Gas Bubbles, *Appl. Therm. Eng.*, **133**: 483–492 (2018). doi:10.1016/j.applthermaleng.2018.01.056.